



Published in final edited form as:

Small. 2014 December 10; 10(23): 4895–4904. doi:10.1002/sml.201400719.

## A Radial Flow Microfluidic Device for Ultra-high-throughput Affinity-based Isolation of Circulating Tumor Cells

**Vasudha Murlidhar,**

Department of Chemical Engineering, University of Michigan, 3074 H.H. Dow 2300 Hayward St.  
Ann Arbor, MI 48109

**Mina Zeinali,**

Department of Chemical Engineering, University of Michigan, 3074 H.H. Dow 2300 Hayward St.  
Ann Arbor, MI 48109

**Svetlana Grabauskiene,**

Department of Surgery, University of Michigan, 1500 E. Medical Center Dr. Ann Arbor, MI 48109

**Mostafa Ghannad-Rezaie, Max S. Wicha,**

Translational Oncology Program, University of Michigan, Ann Arbor, MI

Department of Internal Medicine, University of Michigan Health System, 1500 E. Medical Center  
Drive Ann Arbor, MI 48109

**Diane M. Simeone,**

Department of Surgery, University of Michigan, 1500 E. Medical Center Dr. Ann Arbor, MI 48109

Translational Oncology Program, University of Michigan, Ann Arbor, MI

**Nithya Ramnath,**

Department of Internal Medicine, University of Michigan Health System, 1500 E. Medical Center  
Drive Ann Arbor, MI 48109

**Rishindra M. Reddy, and**

Department of Surgery, University of Michigan, 1500 E. Medical Center Dr. Ann Arbor, MI 48109

**Sunitha Nagrath**

Sunitha Nagrath: [snagrath@umich.edu](mailto:snagrath@umich.edu)

### Abstract

Circulating tumor cells (CTCs) are believed to play an important role in metastasis, a process responsible for the majority of cancer-related deaths. But their rarity in the bloodstream makes microfluidic isolation complex and time-consuming. Additionally the low processing speeds can be a hindrance to obtaining higher yields of CTCs, limiting their potential use as biomarkers for early diagnosis. Here we report a high throughput microfluidic technology, the OncoBean Chip, employing radial flow that introduces a varying shear profile across the device enabling efficient cell capture by affinity at high flow rates. The recovery from whole blood was validated with

---

Correspondence to: Sunitha Nagrath, [snagrath@umich.edu](mailto:snagrath@umich.edu).

Mostafa Ghannad-Rezaie, Present Address: Electrical Engineering Department, Massachusetts Institute of Technology, 77  
Massachusetts Ave. Cambridge, MA 02139

cancer cell lines H1650 and MCF7, achieving a mean efficiency >80% at a throughput of 10 mL hr<sup>-1</sup> in contrast to a flow rate of 1 mL hr<sup>-1</sup> standardly reported with other microfluidic devices. Cells were recovered with a viability rate of 93% at these high speeds, increasing the ability to use captured CTCs for downstream analysis. Broad clinical application was demonstrated using comparable flow rates from blood specimens obtained from breast, pancreatic and lung cancer patients. Comparable CTC numbers were recovered in all the samples at the two flow rates demonstrating the ability of the technology to perform at high-throughputs.

## Keywords

Circulating tumor cells; microfluidics; cancer; high-throughput

## 1. Introduction

Circulating tumor cells (CTCs) have recently gained attention as a useful prognostic tool in cancer patients. They have been identified as useful predictors of metastasis and multiple studies have demonstrated their potential in determining prognosis in metastatic breast, colorectal and prostate cancers.<sup>[1]</sup> Cristofanilli et al. showed that CTCs can predict survival in metastatic breast cancer patients.<sup>[2]</sup> In ovarian cancer, Fan et al. found that stage III/IV (advanced stage) cancer patients exhibited a higher mean CTC count than stage I/II patients, suggesting that elevated numbers of CTCs were present in more advanced stages of disease.<sup>[3]</sup> CTCs are thus useful candidates for clinical monitoring of cancer patients. However, their rarity (1–2 CTCs in 1 mL of blood containing ~10<sup>9</sup> blood cells) prevents important downstream analysis that could provide useful insights into tumor biology and metastasis.<sup>[4–6]</sup> More efficient processing of higher volumes of blood in order to obtain a significant number of these cells thus becomes critical and has the potential to establish the role of CTCs as potential biomarkers for early detection of cancer.

CellSearch is currently the only FDA-approved platform for CTC detection available for clinical use.<sup>[1]</sup> It has successfully demonstrated clinical utility by monitoring CTCs in blood from patients with breast, colon and prostate cancer wherein it was shown that CTCs correlate with poor prognosis.<sup>[1, 7]</sup> CTCs have also been used as investigative biomarkers in clinical trials; two recent clinical trials in lung cancer<sup>[8, 9]</sup> analyzed CTC numbers to predict survival among patients undergoing treatment. Molecular analysis of the CTCs was performed by investigating mutations for primary tumor matching<sup>[8]</sup> or FISH analysis of the CTCs indicating the potential use of CTCs in determining mutation status of patients undergoing therapy.<sup>[9]</sup> CTCs were also investigated in a pancreatic cancer study to evaluate two different technologies for CTC isolation and the possible use of CTCs as a novel biomarker for tumors that are difficult to biopsy.<sup>[10]</sup> Following the initial success of using CTC technologies in predicting patient survival,<sup>[11]</sup> many microfluidic CTC isolation technologies<sup>[4, 5, 7, 12–17]</sup> have been developed to date employing immuno-affinity or physical separation techniques, as they offer a more compact technology with efficient use of resources. While sized-based and other physical separation techniques have been improved to obtain higher throughputs over the years, they suffer from limitations related to the heterogeneity of the tumor cells, contamination with blood cells and result in lower

yields and specificity.<sup>[11]</sup> For example, CTCs within a patient may have a wide range of sizes (>4 to 30  $\mu\text{m}$ ) and many of them may overlap in size with that of the blood cells.<sup>[5]</sup> Affinity-based isolation thus provides a more specific method for CTC enrichment and isolation.

Affinity-based microfluidics operate at low flow rates (1–3  $\text{mL hr}^{-1}$ ) due to shear constraints at high flow rates that may rupture antibody-antigen bonds. The CTC-chip,<sup>[6, 18]</sup> which captures epithelial cancer cells circulating in blood at an operating flow rate of 1  $\text{mL hr}^{-1}$  by using anti-Epithelial Cell Adhesion Molecule (anti-EpCAM) coated on microposts, was the first successful immuno-affinity based microfluidic platform. Subsequently, a second generation platform was developed, known as the Herringbone-Chip (HB-Chip) with a design flow rate of 1.5–2.5  $\text{mL hr}^{-1}$ .<sup>[4]</sup> Gleghorn et al. developed a geometrically enhanced differential immunocapture (GEDI) device that manipulated the flow dynamics around microposts to capture CTCs with high purity at a throughput of 1  $\text{mL hr}^{-1}$ .<sup>[16]</sup> The high throughput microsampling unit (HTMSU) designed by Adams et al. was an integrated device that could both isolate and enumerate CTCs from 1  $\text{mL}$  of blood in about 37 min.<sup>[19]</sup> Many aptamer based technologies were also designed to improve the specificity of capture. One such device was developed by Sheng et al. with a higher flow rate of 600  $\text{nL s}^{-1}$  (or 2.16  $\text{mL hr}^{-1}$ ).<sup>[12]</sup> In 2011, Dickson et al. introduced a device that studied cell lines with different antigen densities for capture at 18  $\mu\text{L min}^{-1}$  (1.08  $\text{mL hr}^{-1}$ ).<sup>[14]</sup> Higher throughputs of isolation have been achieved in subsequent years. An immunomagnetic separation device with a throughput of 10  $\text{mL hr}^{-1}$  was developed by Hoshino et al. in 2011.<sup>[20]</sup> While the throughput is significant for an affinity-based CTC isolation, the sample pre-processing steps such as dilution and centrifugation may lead to cell loss.<sup>[20, 21]</sup> Mittal et al. developed a permeable affinity-capture device operating at 6  $\text{mL hr}^{-1}$  [22] which was subsequently multiplexed to increase throughput.<sup>[23]</sup> More recently, two new integrated platforms were brought forth for CTC isolation. Liu et al. introduced an integrated device that separates blood cells and CTCs by deterministic lateral displacement, followed by an affinity-based enrichment.<sup>[15]</sup> The CTC-iChip by Ozkumur et al. combines inertial focusing with affinity-based capture employing both positive and negative selection.<sup>[7]</sup> The device works by magnetically labeling cancer cells in whole blood, followed by a series of separation steps involving deterministic lateral displacement, inertial focusing and magnetic separation.<sup>[7]</sup> While both these technologies showed a high throughput, 9.6  $\text{mL hr}^{-1}$  and 140  $\mu\text{L/min}$  (or 8.4  $\text{mL hr}^{-1}$ ) respectively,<sup>[7, 15]</sup> the need for multiplexing and pre-processing of blood samples is cumbersome. Labeling of cells in whole blood may also compromise the purity of isolation.<sup>[7]</sup> Processing higher volumes of blood becomes critical from a clinical standpoint as technologies are becoming geared toward single cell mutational analysis of CTCs to monitor patient status.<sup>[8, 9, 24]</sup> Thus, despite advances in the field, a need exists to further improve microfluidics platforms to efficiently monitor and analyze CTCs with minimal pre-processing of blood to preserve these rare cells.

In the exploration for such a device that ensures specificity through antibody-based methods without compromising the volume of blood processed, we developed a radial flow model in contrast to current microfluidic affinity-based capture devices that employ linear flow. We hypothesized that the constant velocity across every cross-section experienced in linear flow based devices is a major limitation for effective capture of cells at higher flow rates. Radial

flow provides an alternative to overcome this drawback as the velocity decreases with increasing cross-sectional area, thereby providing varying shear rates across the radius. Cells would thus experience different shear rates at every radius and would get captured at an optimal shear rate that would be determined by their surface antigen expression. A high surface area for capture was also achieved by designing a bean-shaped micropost with its concave side toward the incoming flow.

We hereby report a radial flow microfluidic device, the OncoBean Chip, inspired by the CTC-chip [6] that efficiently isolates CTCs in one step at high flow rates using an affinity reaction between the Epithelial Cell Adhesion Molecule (EpCAM) antigen expressed by epithelial tumor cells and anti-EpCAM coated on bean-shaped microposts on the microfluidic chip. The OncoBean Chip (Figure 1 A) is designed to operate at a flow rate of  $10 \text{ mL hr}^{-1}$ , capturing rare CTCs through a radial flow design that provides varying shear across the device for optimal capture conditions even at high flow rates.

## 2. Results

### 2.1 Engineering Design and Flow Characteristics

The design of an optimal capture platform with structures relies largely on channelizing the flow in order to have maximum cell contact with functionalized post surfaces. Reducing the flow separation is one way to increase the contact of the cell with the post surfaces, thereby increasing the chance of capture. A circular micropost as in the CTC-chip [6] shows a large flow separation behind the post and the area behind the post remains largely unused for capture. To overcome this, we hypothesized that a bean-shape would provide a better flow utilization for capture. The flow dynamics of a series of different designs of bean-shapes that varied by arc angles and length, followed by a qualitative estimate of boundary layer thickness from fluid simulations was performed using COMSOL Multiphysics 4.2 software.

The OncoBean Chip was designed with bean-shaped posts conceived from an arc angle of  $90^\circ$ , with the structures measuring  $50 \mu\text{m}$  wide and  $118 \mu\text{m}$  along the longest axis. The posts were placed  $25\text{--}32 \mu\text{m}$  apart in polar arrays, with subsequent arrays being rotated to introduce interjection of flow. Figure 1 B, C and D demonstrate velocity magnitude and shear rate profiles on simulated sections. As was expected, for a flow rate of  $10 \text{ mL hr}^{-1}$  the simulations predicted maximum velocity ( $0.0158 \text{ m/s}$ ) for the simulated inlet dimensions and a decreasing trend on moving radially outward as the cross sectional area increased. Similar to the velocity profile, the shear rate decreased on moving toward the outlets. This continuous decrease in shear even at a high flow rate of  $10 \text{ mL hr}^{-1}$  makes it feasible to capture cells with a heterogeneous expression of antigens. A particle trajectory was also simulated to predict hydrodynamic efficiency and to observe streamline paths. The plot (Fig. 1E) shows  $15 \mu\text{m}$  rigid particles and their corresponding streamlines as the particles navigate around the post structures (walls). The simulation predicted 94.3% of particles (33 of 35 particles sent) interact with bean posts within the first  $600 \mu\text{m}$  array of dense posts, with the remaining 2 particles being interjected at other post regions. The simulation thus indicated a high hydrodynamic efficiency and a good streamline trajectory with sufficient cell-post interaction for a sensitive capture.

## 2.2 Optimization of OncoBean Chip for Cancer Cell Capture

The OncoBean Chip was optimized for capture with the epithelial lung cancer cell line H1650 with anti-EpCAM as the capture antibody. Capture efficiency was calculated as the percentage of captured cells on the device to the total number of cells sent, normalized against the OncoBean Chip  $1 \text{ mL hr}^{-1}$  to account for cell spiking errors. Briefly, fluorescently labeled H1650 cells were spiked into healthy blood at a concentration of  $1000 \text{ cells mL}^{-1}$ . To validate the effectiveness of the OncoBean Chip against a standard affinity-based microfluidic device, the OncoBean Chip was compared with a PDMS based version of the CTC Chip (henceforth referred to as the CTC Chip). The following conditions were analyzed: OncoBean Chip  $1 \text{ mL hr}^{-1}$ , OncoBean Chip  $10 \text{ mL hr}^{-1}$ , CTC Chip  $1 \text{ mL hr}^{-1}$  and CTC Chip  $10 \text{ mL hr}^{-1}$ . Upon comparison of performance with the CTC Chip, the OncoBean Chip showed high capture efficiencies with mean yields of 100% and 82.7% at both  $1 \text{ mL hr}^{-1}$  ( $n=4$ ) and  $10 \text{ mL hr}^{-1}$  ( $n=4$ ) respectively (Figure 2 A), in close agreement with the mean capture yield of 90.7% obtained in the CTC Chip at  $1 \text{ mL hr}^{-1}$ . On the other hand, the high capture rate achieved by the CTC Chip at  $1 \text{ mL hr}^{-1}$  dropped to a mean rate of 27.8% with the same chip at a flow rate of  $10 \text{ mL hr}^{-1}$  ( $n=3$ ). This greater than 3-fold drop can be explained by the linear flow profile in the CTC Chip, which may not be conducive for capture at high flow rates due to the high velocities present constantly throughout the device. The OncoBean Chip combats this in its radial flow design as there is a continuous drop in the velocity on moving outward.

The effect of flow rates on the capture efficiency in the OncoBean Chip was tested under four conditions:  $1 \text{ mL hr}^{-1}$ ,  $2.5 \text{ mL hr}^{-1}$ ,  $5 \text{ mL hr}^{-1}$  and  $10 \text{ mL hr}^{-1}$  on anti-EpCAM coated devices to test the robustness of the capture platform at different velocities. As seen in Figure 2 (C) the capture efficiency had no significant drop on increasing the flow rate from 1 to  $10 \text{ mL hr}^{-1}$ , with the mean capture yield being greater than 80% at all the above flow rates. The lowest mean capture efficiency was 89.5% at  $10 \text{ mL hr}^{-1}$  indicating a high yield even at this maximum flow rate. A similar trend in efficiency is observed in the absence of other cells, as is seen in the capture of H1650 cells spiked into serum free medium (shown in Supplementary Figure S1). The OncoBean Chip recovery was also tested with the breast cancer cell line MCF7, and the device achieved a mean capture yield of 98% at  $10 \text{ mL hr}^{-1}$  normalized against the same device at  $1 \text{ mL hr}^{-1}$  at a spike concentration of  $1000 \text{ cells mL}^{-1}$  (Figure 2D). This data suggests that it is possible to obtain similar recovery of CTCs with a process that is 5–10 times faster than many standard affinity isolation methods.

## 2.3 Purity

Non-specific background blood cells are a major hindrance during molecular analysis of CTCs and it is essential not only to achieve effective CTC isolation, but also minimal contamination of these background cells. The purity of capture in the OncoBean Chip was determined by measuring the number of white blood cells (WBCs) per mL of whole blood captured on the device. Due to variations in WBC counts between different donors, a purity percentage was not calculated; a relative comparison caused by increase in flow rates was performed. As shown in Figure 2 (B), the high flow rates tend to have an advantageous effect on reducing the non-specific capture of contaminating WBCs, with a 2-fold drop in the WBC count at  $10 \text{ mL hr}^{-1}$  compared with  $1 \text{ mL hr}^{-1}$  (OncoBean Chip:  $1 \text{ mL hr}^{-1}$  range

1060–1240 cells per mL, 10 mL hr<sup>-1</sup> range 390–740 cells per mL, CTC Chip: 1 mL hr<sup>-1</sup> range 930–2010 cells per mL, 10 mL hr<sup>-1</sup> range 330–850 cells per mL). This may be attributed to the high velocities at high flow rates which reduce the residence time for binding of these cells. The non-specific cell numbers show large variation in capture between the OncoBean and CTC Chips but they indicate similar trends between the flow rates suggesting that the radial gradation in shear does not increase non-specific white blood cell capture.

## 2.4 Cell viability at high flow rates

For optimal use of microfluidic platforms to capture CTCs, cell viability is an important readout as it determines the feasibility of performing critical downstream assays on CTCs, such as genetic profiling.<sup>[25]</sup> Since high flow rates can induce high shear rates which can be detrimental to cell health,<sup>[6]</sup> the cell viability was assessed in the OncoBean platform using the Invitrogen Live/Dead Assay. Briefly, H1650 cells were spiked into serum free medium and processed through anti-EpCAM coated OncoBean Chip at a flow rate of 10 mL hr<sup>-1</sup>. Live/Dead reagent was flushed through the device and incubated for 15 minutes, followed by microscopic imaging of several 10x magnification fields of view. The first four fields of view were considered as accurate estimates of cell viability. Live and dead cells were manually counted in a blinded manner and cell viability was defined as the percent ratio of number of cells alive to the total number of cells in the field of view. Using this assay, 92.91 ± 1.63% (mean ± s.d.) of the cells were found to be viable after flow at high throughput, comparable to the mean viability of 98.5% reported for the CTC Chip.<sup>[6]</sup> These data indicate that despite facing an initial momentary high stress at higher flow rates, cell viability is not diminished compared to lower flow rates, perhaps due to the continuous drop in shear stress that is produced by the radial flow (Figure S4).

## 2.5 Capture profile

The varying shear stress model proposed in the OncoBean chip suggests there are differential regions of capture on the OncoBean, dependent on antigen density. For a given flow rate, capture of a high EpCAM expressing cell would require less residence time for binding than a low EpCAM expressing cell.<sup>[22, 26, 27]</sup> This translates to distance traversed within the device, or the number of antibody-coated posts encountered by the cell. At low flow rates, the cells would be captured within a small distance into the device due to the radial drop in shear in addition to the already-low shear rates. At high flow rates, a larger capture distance is required as the velocity needs to slow down sufficiently for the cells to bind. To test this hypothesis, H1650 cells were spiked into serum free medium and captured at 1 mL hr<sup>-1</sup> and 10 mL hr<sup>-1</sup>. The cells captured were manually counted at 1000 µm radial intervals. The capture profile plot (Figure 2 E and F) shows the distribution of captured cells along various radial positions in the OncoBean Chip. It was observed that with H1650, a cell line with high EpCAM expression (greater than 500,000 antigens per cell),<sup>[6]</sup> most cells are captured within the first half radius of the device at 1 mL hr<sup>-1</sup> (Figure 2 E), while the capture is more widespread at 10 mL hr<sup>-1</sup> (Figure 2 F), utilizing a larger area of the device at the higher flow rate. This was in accordance with our predictions. A similar capture profile was observed for MCF7 cells as well.



## 2.6 CTC Capture in Cancer Patients

The strength of the technology was assessed by testing clinical specimens from different cancers. Whole blood from healthy donors ( $n = 4$ ) was processed as controls at  $10 \text{ mL hr}^{-1}$  to test for the specificity of capture against anti-EpCAM. After fixation of the cells on the device, the cells were permeabilized and stained for anti-Cytokeratin (CK) (tumor specific epithelial marker), anti-CD45 (leukocyte marker) and DAPI (nuclear stain) and respective secondary antibodies for immunofluorescent imaging. The criteria for CTC enumeration was a CK+, CD45- and DAPI+ expression profile.<sup>[6]</sup> The healthy controls gave a recovery of  $1.4 \pm 0.89$  CTCs per mL (range  $0.91\text{--}2.67$  CTCs per mL, median  $1.13$  CTCs per mL) as per the above enumeration criteria (supplementary figure S3). Following this, a threshold of 2 CTCs per mL was set for CTC detection in clinical specimens.<sup>[28]</sup> Whole blood from pancreatic ( $n = 2$ ), breast ( $n = 2$ ) and lung ( $n = 2$ ) cancer patients were processed through the OncoBean Chip at  $1$  and  $10 \text{ mL hr}^{-1}$  in equal volumes to observe CTC recovery using an anti-EpCAM antibody. According to this criteria, CTCs were detected by the device in 100% of the samples, with a recovery of  $4.2 \pm 0.65$  CTCs per mL at  $1 \text{ mL hr}^{-1}$  (range  $3.33\text{--}5$  CTCs per mL, median  $4$  CTCs per mL) and  $4.33 \pm 0.85$  CTCs per mL at  $10 \text{ mL hr}^{-1}$  (range  $3\text{--}5$  CTCs per mL, median  $4.67$  CTCs per mL). The high flow rate of  $10 \text{ mL hr}^{-1}$  gave equivalent recovery in 5 of 6 samples. Because of the small cohort of specimens tested, statistical significance was not observed. The CTC yields across the different cancers at the two flow rates are shown in Figure 4A. It can be seen that the high flow rate has a similar CTC recovery capacity to that at a low flow rate in the various cancer specimens processed.

## 3. Discussions and Conclusion

High throughput analysis has remained a major hurdle in the retrieval of circulating tumor cells from cancer patients and is a critical issue in the development of new microfluidic technologies to measure CTCs.<sup>[25]</sup> While many physical separation methods and integrated systems have been developed, to our knowledge, no affinity-based one-step cell recovery technologies have yet been developed for high throughput analysis. The OncoBean Chip is a first immuno-enrichment technique of its kind offering the specificity of antibody-based capture in a high throughput manner ( $10 \text{ mL hr}^{-1}$ ). It works by isolating CTCs from whole blood in a single step, without the need for pre-processing or dilutions. It achieves its high throughput functionality through a simple technique of a radial flow channel. Fluid simulations and theoretical calculations show that the fluid velocity in the radial flow OncoBean Chip varies as  $1/(2\pi rh)$ , where  $r$  and  $h$  stand for the radius and height of the channels, respectively. While increasing the height of the channel is an alternative to achieving high throughput, microfabrication of a high aspect ratio channel might be challenging. A flow profile which dynamically varies with distance thus offers an economical and compact technology that enables the processing of high volumes of fluid samples, which is highly advantageous in the context of rare circulating tumor cells. The design of the OncoBean Chip is thus optimal for this purpose, as it achieves an average capture efficiency ( $>80\%$ ) comparable to that of the CTC Chip, which still remains a benchmark for microfluidic CTC extraction by immuno-affinity methods.<sup>[5, 11]</sup>

Immuno-affinity based microfluidic platforms like the CTC Chip and others perform poorly at high flow rates due to the linear flow profile wherein many cells either escape the substrate interactions or are travelling at a constantly high velocity throughout the device in order for binding to occur.<sup>[4, 6]</sup> The OncoBean Chip shows stable binding at high flow rates due to the drop in velocity at every radial position toward the outlets. Reducing shear at different cross sections in the chip also allows a high flow rate without compromising cell viability, increasing the feasibility of downstream processing of these cells to obtain molecular characteristics and genetic information.<sup>[25, 29]</sup>

While high volumes of blood used for CTC analysis potentially offer higher yields of these rare cells, the detection methods also face the issue of an increased background contamination owing to the quantity of sample. We observed that WBC contamination was not a major concern in the OncoBean Chip as the high velocities prevented high non-specific binding. There is a greater than 2-fold drop in the contaminating WBCs when run at 10 mL hr<sup>-1</sup> in contrast to 1 mL hr<sup>-1</sup> (Figure 2 B), and also a continuous drop in non-specific binding with increasing flow rates. This is expected as the higher velocities reduce the interaction time of these non-specific cells with the tumor-specific-antibody coated posts, thereby reducing contamination. The higher levels of purity coupled with higher CTC yields in a one-step strategy should enhance accuracy in molecular analyses of the recovered CTC population.<sup>[30]</sup>

Affinity-based microfluidics are dependent on antibody-antigen kinetics, and antigen density is an important parameter controlling the rate of capture.<sup>[22, 26, 27]</sup> The capture profile plot (Figure 2) shows that a cell with high EpCAM expression such as H1650 would be captured early in the device as the antigen density would enhance bond formation, whereas a cell with lower EpCAM expression would be concentrated around the latter half of the device, nearer to the outlets, as the cells would need to be at a sufficiently lower velocity for binding to occur due to the smaller number of binding sites.<sup>[22, 26]</sup> The OncoBean is thus conducive to capturing cells with a wide range of EpCAM antigen expression. It is also possible that multiple antibody combinations could be used in the OncoBean Chip in the future to further fine tune CTC capture.

As with all diagnostic technologies, bench-to-bedside remains the deciding factor for the device's competence. The OncoBean Chip shows initial promise with clinical samples, capturing CTCs from the blood of patients with epithelial cancers by the use of anti-EpCAM as the capture antibody. Out of the 6 patient samples tested, 5 show equivalent capture at 10 mL hr<sup>-1</sup> compared to capture at 1 mL hr<sup>-1</sup>. This demonstrates the potential of this technology as a high-throughput platform to evaluate CTCs in different cancers. The technology also enables the processing of 7.5 mL of blood in under an hour, which is not only unprecedented in many other microfluidic technologies, but also attractive from a clinician's perspective. The OncoBean Chip is thus a potential tool for blood based diagnostics that can quickly become part of routine clinical tests. The healthy controls also indicate the specificity of capture by this technique. Although the small cohort of patients and the volume of blood processed for unbiased comparison with that at low flow rate restrict a rigorous sensitivity analysis of the device, the capture efficiency of the device shows potential for using higher volumes of blood for recovery of higher CTC numbers.



While a few high throughput affinity isolation technologies have recently been developed, they invariably require working with diluted blood, or multiplexing and integration of devices.<sup>[7, 15, 20, 22, 23]</sup> Also, immunomagnetic technologies suffer from limitations such as reduction in the binding affinities of antibodies on magnetic particles, requiring higher amounts of antibodies to screen larger cell populations.<sup>[21, 31]</sup> Tumor heterogeneity brings forth another set of challenges for physical separations as CTCs are observed to be widely different, with size heterogeneity being the most evident.<sup>[25, 32, 33]</sup> Hou et al. witnessed a range of 10–22.5  $\mu\text{m}$  in the CTC sizes isolated using their physical separation device.<sup>[32]</sup> While many such devices perform at commendable throughputs, such size variations may result in significant CTC loss.

We have thus shown that high-throughput processing with immuno-affinity capture is possible even without multiplexing such as in physical separations which in many cases involve complex handling to reduce the blood volume.<sup>[7, 15]</sup> We have validated the efficacy of the technology with cancer cell lines and also with clinical specimens. In addition, it has also been shown that the ultra-high throughput used is not detrimental to the cell viability, yields good purity and can be capitalized for downstream studies. The major highlight of the OncoBean Chip lies in its design of radial flow, which can be easily incorporated into other microfluidic chips, such as the graphene oxide chip developed by our group<sup>[28]</sup> and other devices that may be utilized for CTC culture. The captured cells can be released by widely used cell recovery techniques as described in<sup>[13, 19]</sup> or by incorporating thin coating of hydrogels as shown by Shah et al.<sup>[34]</sup> The OncoBean Chip would thus be useful in the cases of early stage cancers where there may not be sufficient number of cells in the circulation in order to be detected in 1–3 mL of blood and thus shows great promise as an early diagnostic tool.

## 4. Experimental Section

### COMSOL Simulations

Finite element simulations were performed in COMSOL Multiphysics 4.2 (Comsol Inc.) with an inlet flow rate of  $10 \text{ mL hr}^{-1}$  on a 6 mm radial section and  $30^\circ$  arc of the proposed device. Navier-Stokes equations for incompressible fluid flow were used for the study. A symmetry boundary condition was applied on the two similar boundaries flanking the posts. Wall (no slip) boundary condition was applied on the post outlines. The particle tracing plot was simulated with rigid particles  $15 \mu\text{m}$  in size, with a condition of sticking to any encountered wall being applied.

### Device fabrication

The design was prepared using AutoCAD software with the following dimensions: bean width  $50 \mu\text{m}$ , arc angles  $90^\circ$ , adjacent (lateral) post spacing  $25\text{--}32 \mu\text{m}$ . The design was converted to a photomask (FineLine Imaging) and used to prepare a mold by traditional photolithography. Briefly, a negative photoresist SU-8 100 (MicroChem Corp) was spin coated onto a silicon wafer at 2350 rpm. This was followed by soft baking at  $65^\circ\text{C}$  for 10 min and  $95^\circ\text{C}$  for 70 min, and then UV exposure of the pattern onto the wafer for 15 sec. Post exposure baking was done at  $65^\circ\text{C}$  for 3 min and  $95^\circ\text{C}$  for 10 min and the pattern was

developed in SU-8 developer. The wafer was then hard baked at 150 °C for 3 min. A post height of 100 µm was achieved. Poly-dimethoxysilane or PDMS (Ellsworth Adhesives) was prepared in a monomer to curing agent ratio of 10:1 and baked overnight after degassing. The PDMS was peeled from the master mold, cut and prepared for surface modification.

Each PDMS chip was bonded onto a glass slide using plasma bonding. 3-mercaptopropyltrimethoxy silane (Gelest) was infused and incubated for 1 hour. This was followed by washing with ethanol and addition of N-gamma-Maleimidobutyryloxy-Succinimide (GMBS) (ThermoScientific), a cross linking agent for 30 mins. The devices were washed again and Neutravidin (Invitrogen-Life Technologies Inc.) was added and the devices were stored at 4 °C. Before experiments, the devices were incubated with biotin-conjugated anti-EpCAM (RnD Systems).

### Cell preparation

Human lung cancer cell line H1650 and human breast cancer cell line MCF7 were cultured in RPMI-1640 and DMEM (Invitrogen - LifeTechnologies, Inc.) respectively. The media were supplemented with 10% fetal bovine serum (Invitrogen - LifeTechnologies, Inc.). Both additionally contained 1% antibiotic-antimycotic solution. Cells were grown at 37 °C and 5% CO<sub>2</sub> and medium was renewed every 2–3 days. Cells were passaged with 0.05% Trypsin-0.53 mM EDTA (Invitrogen - LifeTechnologies, Inc.).

### Cell capture and analysis

The cells were harvested with 0.05% Trypsin-0.53 mM EDTA and labeled with CellTracker Green fluorescent dye (Invitrogen - LifeTechnologies, Inc.). They were counted with a hemocytometer and spiked into healthy blood or serum free medium. Informed consent was obtained from all healthy blood donors. The devices were incubated with anti-EpCAM prior to experiments. After antibody immobilization and wash, low dead volume tubing from Cole-Parmer (AAD02091-CP) was connected to the device and flow was facilitated through a syringe needle. 3% bovine serum albumin (Sigma Aldrich) was used as a blocking agent to reduce non-specific binding. Two of the three outlets in the device were connected by a short tubing to have a single outlet port for waste blood collection, while also increasing the fluid resistance. The fluid spiked with known number of cells was then processed through the device at the respective flow rates. This was followed by washing with phosphate buffer saline (PBS) and fixing and permeabilization with BD Cytotfix/Cytoperm (BD Biosciences). DAPI (4',6-diamidino-2-phenylindole) (Invitrogen - LifeTechnologies, Inc.) was then applied to stain the nucleus followed by a last washing step. The devices were stored at 4 °C until visualization with Nikon Eclipse Ti fluorescence microscope.

Statistical analysis was performed with the software OriginPro 9.0. A standard two-sample t-test was used for comparison between the groups.

### Patient CTC analysis

Informed consent was obtained from all donors. Whole blood from cancer patients was processed through the OncoBean Chip at the designated flow rates in equal volumes, followed by washing with phosphate buffer saline. The cells were fixed with 4%

paraformaldehyde and refrigerated at 4 °C until immunofluorescent staining. Before staining, the cells were permeabilized with 0.2% Triton-X 100, followed by blocking with 2% goat serum in 3% bovine serum albumin. Primary antibodies anti-Cytokeratin 7/8 (BD Biosciences) and anti-CD45 (BD Biosciences) were applied in 1% bovine serum albumin for all samples with the exception of pancreatic cancer specimens where anti-Cytokeratin 19 (SantaCruz Biotechnology Inc.) and anti-CD45 (SantaCruz Biotechnology Inc.) were used. After a quick wash, secondary antibodies AlexaFluor 488 and AlexaFluor 546 or 568 (Invitrogen-Life Technologies Inc.) were applied in 1 % bovine serum albumin. DAPI was applied as the final step before microscopic imaging.

### Cell viability assay

H1650 cells were harvested and spiked into serum free RPMI 1640 and processed through the OncoBean Chip at 10 mL hr<sup>-1</sup>. The live/dead reagent consisting of calcein AM and ethidium homodimer<sup>-1</sup> (Invitrogen - LifeTechnologies, Inc.) was prepared as specified by manufacturer and applied to the cells in the device. Following 15 min of incubation, several fields of view were microscopically imaged under 10x magnification.

### Supplementary Material

Refer to Web version on PubMed Central for supplementary material.

### Acknowledgements

This work was supported by the National Institutes of Health (NIH) Director's New Innovator Award (1DP2OD006672-01), a Career Development Program of the Gastrointestinal Specialized Program of Research Excellence (GI SPORE) award (CA 130810), and a Department of Defense (DoD) Office of the Congressionally Directed Medical Research Programs (CDMRP) Career Development Award to S. Nagrath. The authors would like to thank Dr. Nikos Chronis, and the clinical specimen coordinators Dr. Shari Barnett, Stephanie Laurinec, Heather Cameron, Dr. Monica Burness and Jill Hayden. The authors also acknowledge the Lurie Nanofabrication Facility and the Microscopy and Image Analysis (MIL) facility of the University of Michigan.

### References

1. Miller MC, Doyle GV, Terstappen LW. Journal of oncology. 2010; 2010:617421. [PubMed: 20016752]
2. Cristofanilli M, Budd GT, Ellis MJ, Stopeck A, Matera J, Miller MC, Reuben JM, Doyle GV, Allard WJ, Terstappen LW, Hayes DF. The New England journal of medicine. 2004; 351(8):781–791. [PubMed: 15317891]
3. Fan T, Zhao Q, Chen JJ, Chen WT, Pearl ML. Gynecologic oncology. 2009; 112(1):185–191. [PubMed: 18954898]
4. Stott SL, Hsu CH, Tsukrov DI, Yu M, Miyamoto DT, Waltman BA, Rothenberg SM, Shah AM, Smas ME, Korir GK, Floyd FP Jr, Gilman AJ, Lord JB, Winokur D, Springer S, Irimia D, Nagrath S, Sequist LV, Lee RJ, Isselbacher KJ, Maheswaran S, Haber DA, Toner M. Proceedings of the National Academy of Sciences of the United States of America. 2010; 107(43):18392–18397. [PubMed: 20930119]
5. Dong Y, Skelley AM, Merdek KD, Sprott KM, Jiang C, Pierceall WE, Lin J, Stocum M, Carney WP, Smirnov DA. The Journal of molecular diagnostics : JMD. 2013; 15(2):149–157. [PubMed: 23266318]
6. Nagrath S, Sequist LV, Maheswaran S, Bell DW, Irimia D, Ulkus L, Smith MR, Kwak EL, Digumarthy S, Muzikansky A, Ryan P, Balis UJ, Tompkins RG, Haber DA, Toner M. Nature. 2007; 450(7173):1235–1239. [PubMed: 18097410]

7. Ozkumur E, Shah AM, Ciciliano JC, Emmink BL, Miyamoto DT, Brachtel E, Yu M, Chen PI, Morgan B, Trautwein J, Kimura A, Sengupta S, Stott SL, Karabacak NM, Barber TA, Walsh JR, Smith K, Spuhler PS, Sullivan JP, Lee RJ, Ting DT, Luo X, Shaw AT, Bardia A, Sequist LV, Louis DN, Maheswaran S, Kapur R, Haber DA, Toner M. *Science translational medicine*. 2013; 5(179): 179ra47.
8. Punnoose EA, Atwal S, Liu W, Raja R, Fine BM, Hughes BG, Hicks RJ, Hampton GM, Amler LC, Pirzkall A, Lackner MR. *Clinical cancer research : an official journal of the American Association for Cancer Research*. 2012; 18(8):2391–2401. [PubMed: 22492982]
9. Rudin CM, Hann CL, Garon EB, Ribeiro de Oliveira M, Bonomi PD, Camidge DR, Chu Q, Giaccone G, Khaira D, Ramalingam SS, Ranson MR, Dive C, McKeegan EM, Chyla BJ, Dowell BL, Chakravarty A, Nolan CE, Rudersdorf N, Busman TA, Mabry MH, Krivoschik AP, Humerickhouse RA, Shapiro GI, Gandhi L. *Clinical cancer research : an official journal of the American Association for Cancer Research*. 2012; 18(11):3163–9. [PubMed: 22496272]
10. Khoja L, Backen A, Sloane R, Menasce L, Ryder D, Krebs M, Board R, Clack G, Hughes A, Blackhall F, Valle JW, Dive C. *British journal of cancer*. 2012; 106(3):508–516. [PubMed: 22187035]
11. Sun YF, Yang XR, Zhou J, Qiu SJ, Fan J, Xu Y. *Journal of cancer research and clinical oncology*. 2011; 137(8):1151–1173. [PubMed: 21681690]
12. Sheng W, Chen T, Kamath R, Xiong X, Tan W, Fan ZH. *Analytical chemistry*. 2012; 84(9):4199–4206. [PubMed: 22482734]
13. Dharmasiri U, Balamurugan S, Adams AA, Okagbare PI, Obubuafo A, Soper SA. *Electrophoresis*. 2009; 30(18):3289–3300. [PubMed: 19722212]
14. Nora Dickson M, Tsinberg P, Tang Z, Bischoff FZ, Wilson T, Leonard EF. *Biomicrofluidics*. 2011; 5(3):34119–3411915. [PubMed: 22662044]
15. Liu Z, Zhang W, Huang F, Feng H, Shu W, Xu X, Chen Y. *Biosensors & bioelectronics*. 2013; 47:113–119. [PubMed: 23567630]
16. Gleghorn JP, Pratt ED, Denning D, Liu H, Bander NH, Tagawa ST, Nanus DM, Giannakakou PA, Kirby BJ. *Lab on a chip*. 2010; 10(1):27–29. [PubMed: 20024046]
17. Paterlini-Brechot P, Benali NL. *Cancer letters*. 2007; 253(2):180–204. [PubMed: 17314005]
18. Sequist LV, Nagrath S, Toner M, Haber DA, Lynch TJ. *Journal of thoracic oncology : official publication of the International Association for the Study of Lung Cancer*. 2009; 4(3):281–283.
19. Adams AA, Okagbare PI, Feng J, Hupert ML, Patterson D, Gottert J, McCarley RL, Nikitopoulos D, Murphy MC, Soper SA. *Journal of the American Chemical Society*. 2008; 130(27):8633–8641. [PubMed: 18557614]
20. Hoshino K, Huang YY, Lane N, Huebschman M, Uhr JW, Frenkel EP, Zhang X. *Lab on a chip*. 2011; 11(20):3449–3457. [PubMed: 21863182]
21. Karabacak NM, Spuhler PS, Fachin F, Lim EJ, Pai V, Ozkumur E, Martel JM, Kojic N, Smith K, Chen PI, Yang J, Hwang H, Morgan B, Trautwein J, Barber TA, Stott SL, Maheswaran S, Kapur R, Haber DA, Toner M. *Nature protocols*. 2014; 9(3):694–710. [PubMed: 24577360]
22. Mittal S, Wong IY, Deen WM, Toner M. *Biophysical journal*. 2012; 102(4):721–730. [PubMed: 22385842]
23. Mittal S, Wong IY, Yanik AA, Deen WM, Toner M. *Small*. 2013; 9(24):4207–4214. [PubMed: 23766297]
24. Powell AA, Talasaz AH, Zhang H, Coram MA, Reddy A, Deng G, Telli ML, Advani RH, Carlson RW, Mollick JA, Sheth S, Kurian AW, Ford JM, Stockdale FE, Quake SR, Pease RF, Mindrinos MN, Bhanot G, Dairkee SH, Davis RW, Jeffrey SS. *PloS one*. 2012; 7(5):e33788. [PubMed: 22586443]
25. den Toonder J. *Lab on a chip*. 2011; 11(3):375–377. [PubMed: 21206959]
26. Zheng X, Cheung LS, Schroeder JA, Jiang L, Zohar Y. *Lab on a chip*. 2011; 11(19):3269–3276. [PubMed: 21837324]
27. Mikolajczyk SD, Millar LS, Tsinberg P, Coutts SM, Zomorodi M, Pham T, Bischoff FZ, Pircher TJ. *Journal of oncology*. 2011; 2011:252361. [PubMed: 21577258]
28. Yoon HJ, Kim TH, Zhang Z, Azizi E, Pham TM, Paoletti C, Lin J, Ramnath N, Wicha MS, Hayes DF, Simeone DM, Nagrath S. *Nature nanotechnology*. 2013; 8(10):735–741.

29. Smirnov DA, Zweitzig DR, Foulk BW, Miller MC, Doyle GV, Pienta KJ, Meropol NJ, Weiner LM, Cohen SJ, Moreno JG, Connelly MC, Terstappen LW, O'Hara SM. Cancer research. 2005; 65(12):4993–4997. [PubMed: 15958538]
30. Maheswaran S, Sequist LV, Nagrath S, Ulkus L, Brannigan B, Collura CV, Inserra E, Diederichs S, Iafrate AJ, Bell DW, Digumarthy S, Muzikansky A, Irimia D, Settleman J, Tompkins RG, Lynch TJ, Toner M, Haber DA. The New England journal of medicine. 2008; 359(4):366–377. [PubMed: 18596266]
31. Zhang H, Williams PS, Zborowski M, Chalmers JJ. Biotechnology and bioengineering. 2006; 95(5):812–829. [PubMed: 16937410]
32. Hou HW, Warkiani ME, Khoo BL, Li ZR, Soo RA, Tan DS, Lim WT, Han J, Bhagat AA, Lim CT. Scientific reports. 2013; 3:1259. [PubMed: 23405273]
33. Hou JM, Krebs M, Ward T, Sloane R, Priest L, Hughes A, Clack G, Ranson M, Blackhall F, Dive C. The American journal of pathology. 2011; 178(3):989–996. [PubMed: 21356352]
34. Shah AM, Yu M, Nakamura Z, Ciciliano J, Ulman M, Kotz K, Stott SL, Maheswaran S, Haber DA, Toner M. Analytical chemistry. 2012; 84(8):3682–3688. [PubMed: 22414137]

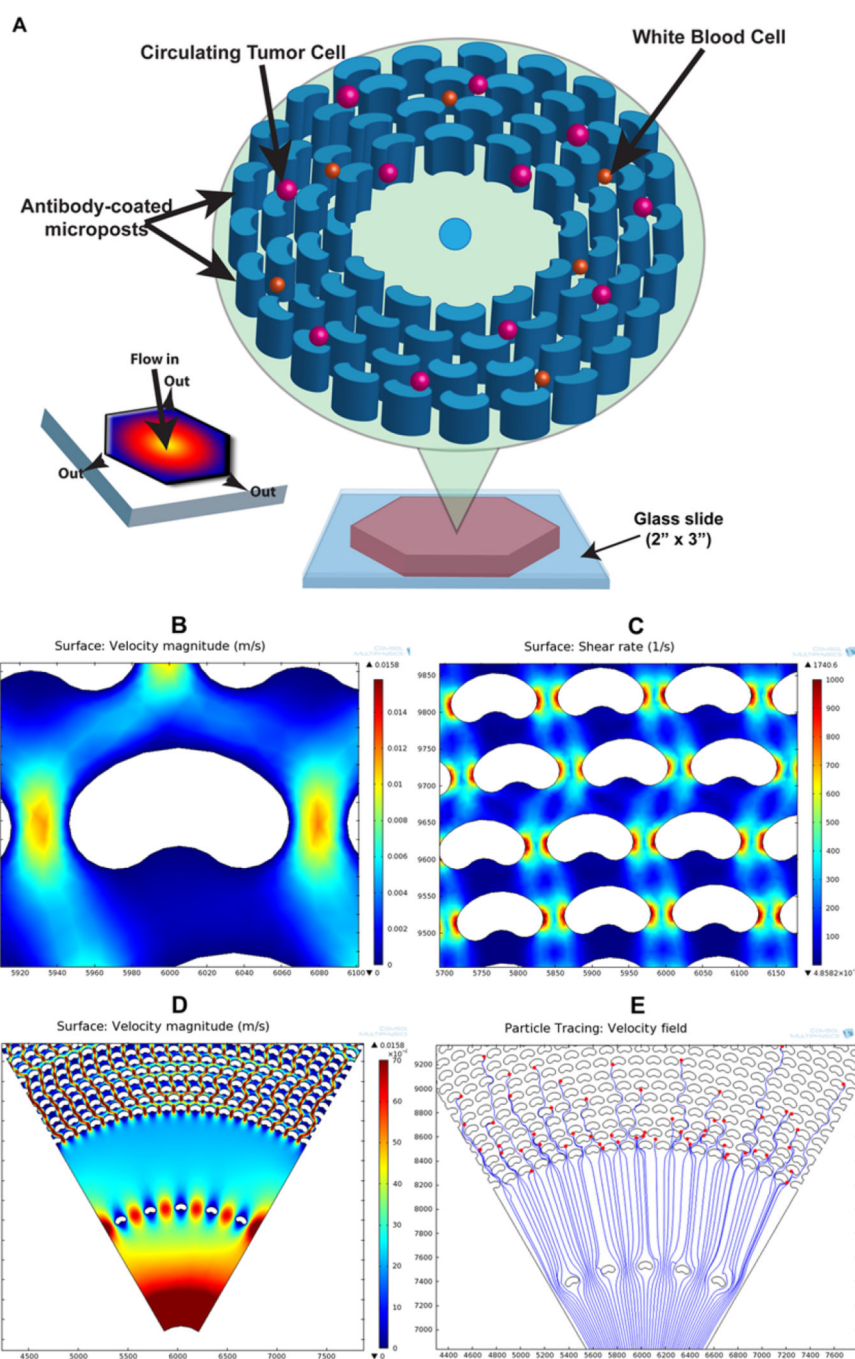


**Figure 1. Schematic representation of OncoBean Chip and finite element simulations**  
 (A) Schematic representation of the OncoBean Chip shows cancer cells (pink) being captured on antibody coated bean-shaped microposts. Inset shows a flow profile representation with velocity decreasing from red to blue. Finite element simulations on a section of the OncoBean Chip show (B) velocity magnitude of flow around a single post (magnified image) and flow converging behind the post, (C) surface plot of shear rate around the posts indicating slowing down of flow near the post face (concave side) (D) velocity magnitude profile across posts near the inlet (bottom arc) (E) particle tracing plot



around microposts near the inlet demonstrating typical streamlines (blue) and capture of 15  $\mu\text{m}$  rigid particles (red) upon encountering a wall (post). Flow occurs from bottom toward top in these images.

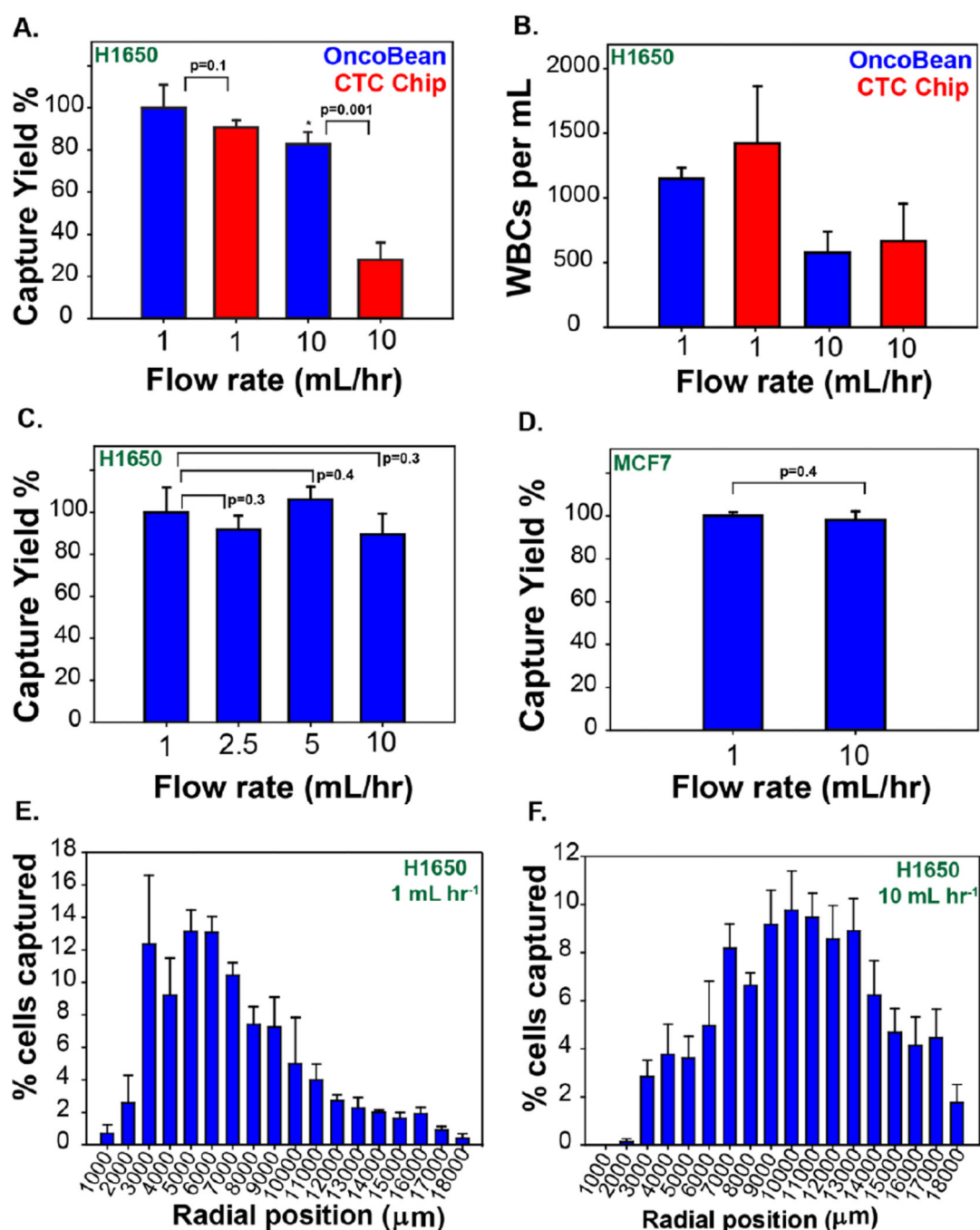


**Figure 2. Optimization of capture efficiency**

(A) Comparison of H1650 cell capture from whole blood between OncoBean Chip vs CTC Chip at 1 and 10 mL hr<sup>-1</sup> normalized to OncoBean Chip at 1 mL hr<sup>-1</sup> (B) Non-specific white blood cell capture for the experiment in (A) represented as the number of white blood cells per mL of whole blood. (C) Effect of flow rates on capture of H1650 cells spiked into whole blood by the OncoBean Chip shows capture yields at 1, 2.5, 5 and 10 mL hr<sup>-1</sup> (D) Capture of MCF7 cells from whole blood by the OncoBean Chip at 1 and 10 mL hr<sup>-1</sup> (E) and (F) show capture profile or position of H1650 cells captured from serum free medium

across different radial distances along the OncoBean Chip at  $1 \text{ mL hr}^{-1}$  and  $10 \text{ mL hr}^{-1}$  respectively.

Author Manuscript

Author Manuscript

Author Manuscript

Author Manuscript

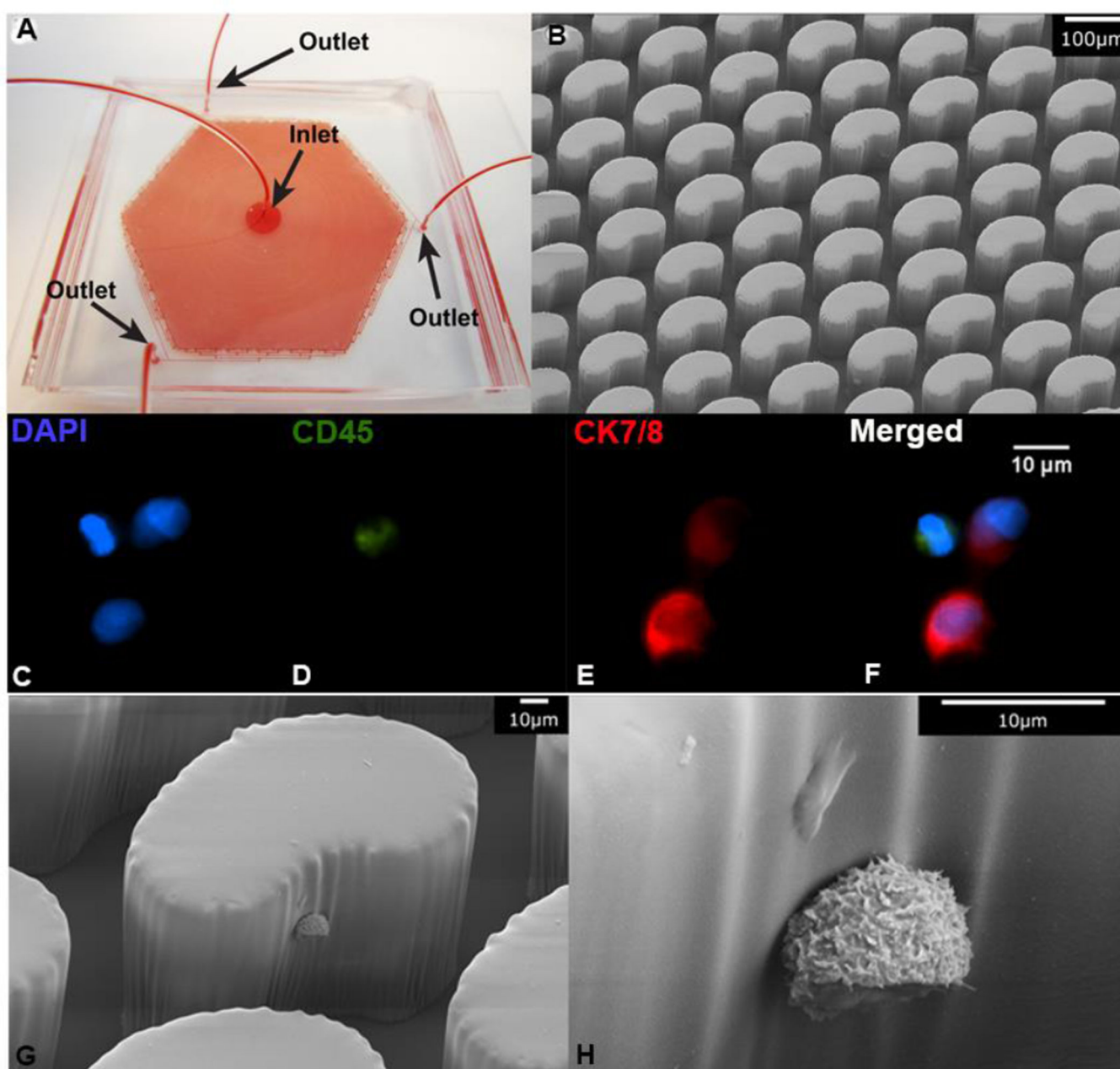


**Figure 3. Cell capture on the OncoBean Chip**

(A). The OncoBean Chip with blood flow shows inlet and outlet positions (B) Scanning electron micrograph of the device shows bean-shaped micropost structures. H1650 cells in blood captured by the OncoBean Chip: panel shows immunofluorescence images of cells stained for nucleus with DAPI (C), CD45 – a white blood cell marker (D), cytokeratin 7–8 that stains the H1650 cancer cells (E), and a merged field (F) showing all fluorescent stains. (G) is a scanning electron micrograph of a H1650 cell captured on a bean-shaped micropost, with (H) showing a magnified view of the cell.

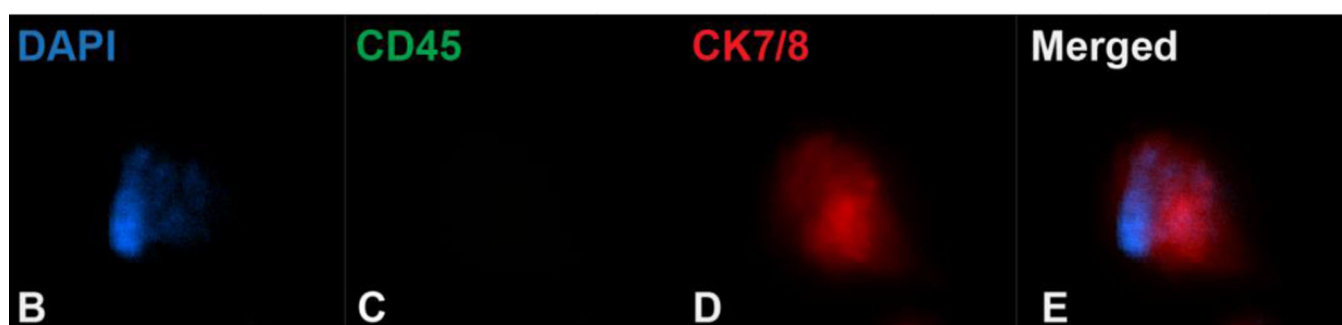
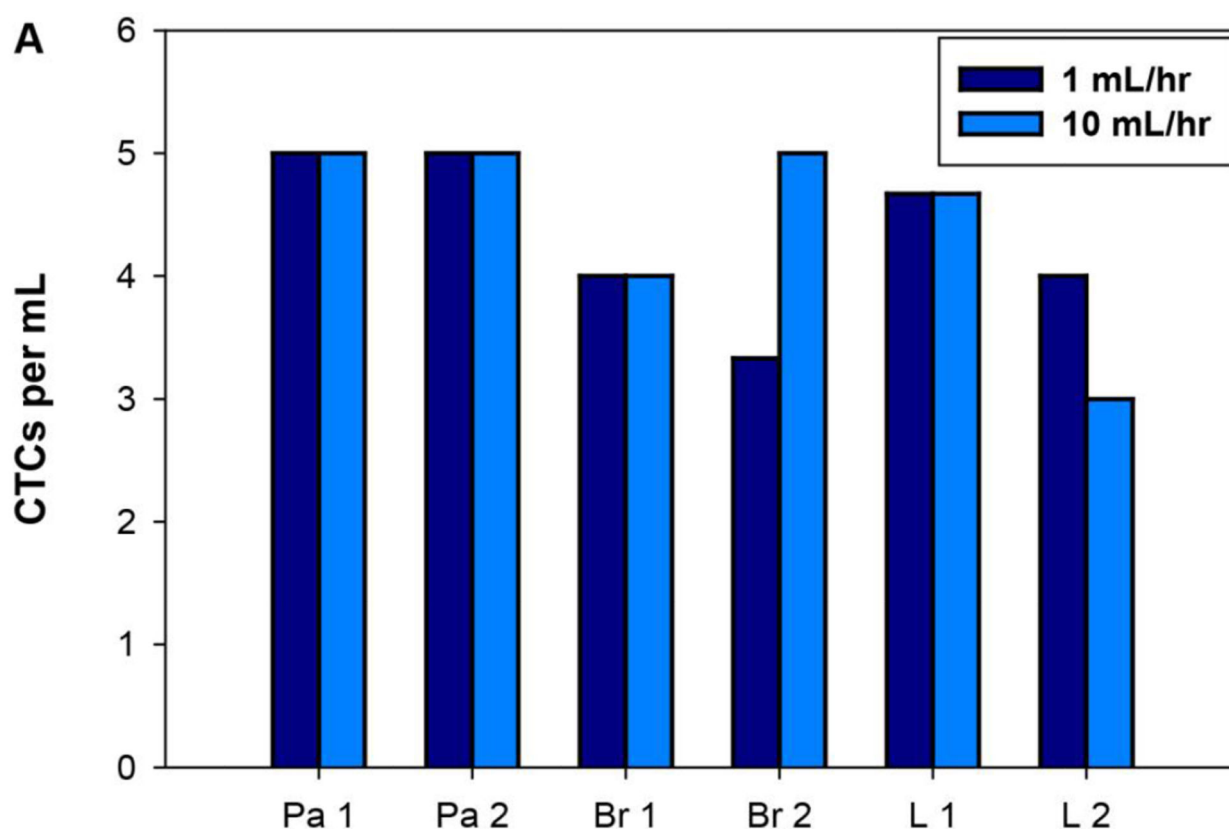


**Figure 4. OncoBean Chip validation with patient samples**

(A). Clinical performance of the OncoBean Chip showing CTC recovery from patients with pancreatic (Pa), breast (Br) and lung cancer (L) at 1 and 10 mL hr<sup>-1</sup>. Panel at the bottom shows immunofluorescent staining of a lung CTC recovered at 10 mL hr<sup>-1</sup> showing (B) nucleus, (C) absence of CD45, (D) cytokeratin 7/8 and (E) a merged field with all channel staining.